IEEE Access
Multidisciplinary ⋮ Rapid Review ⋮ Open Access Journal

Received 27 January 2024, accepted 19 February 2024, date of publication 26 February 2024, date of current version 8 March 2024.

Digital Object Identifier 10.1109/ACCESS.2024.3370860

RESEARCH ARTICLE

Dual-Polarized Wideband 5G N77 Band Slotted MIMO Antenna System for Next-Generation Smartphones

SAAD HASSAN KIANI[1,2], MEHR E. MUNIR[3], HÜSEYIN ŞERIF SAVCI[1], (Senior Member, IEEE), HATEM RMILI[2], (Senior Member, IEEE), EATEDAL ALABDULKREEM[4], HELA ELMANNAI[5], GIOVANNI PAU[6], (Senior Member, IEEE), AND MOHAMMAD ALIBAKHSHIKENARI[7], (Member, IEEE)

[1]Electrical and Electronics Engineering Department, RFMicroSense Research Group, Istanbul Medipol University, 34810 İstanbul, Turkey
[2]Electrical and Computer Engineering Department, Faculty of Engineering, King Abdulaziz University, Jeddah 23513, Saudi Arabia
[3]Smart Systems Engineering Laboratory, College of Engineering, Prince Sultan University, Riyadh 11586, Saudi Arabia
[4]Department of Computer Science, College of Computer and Information Science, Princess Nourah bint Abdulrahman University, P.O. Box 84428, Riyadh 11671, Saudi Arabia
[5]Department of Information Technology, College of Computer and Information Science, Princess Nourah bint Abdulrahman University, P.O. Box 84428, Riyadh 11671, Saudi Arabia
[6]Faculty of Engineering and Architecture, Kore University of Enna, 94100 Enna, Italy
[7]Department of Signal Theory and Communications, Universidad Carlos III de Madrid, Leganés, 28911 Madrid, Spain

Corresponding authors: Hüseyin Şerif Savci (hsavci@medipol.edu.tr), Giovanni Pau (giovanni.pau@unikore.it), and Mohammad Alibakhshikenari (mohammad.alibakhshikenari@uc3m.es)

This work was supported by Princess Nourah bint Abdulrahman University Researchers Supporting Projectnumbr (PNURSP2024R161), Princess Nourah bint Abdulrahman University, Riyadh, Saudi Arabia and by the Deanship of Scientific Research (DSR) funded by King Abdulaziz University, Jeddah, under Grant RG-13-135-43. The authors would also like to acknowledge the support of Prince Sultan University, Riyadh, Saudi Arabia for providing funding for this article. Besides above, Dr. Mohammad Alibakhshikenari acknowledges support from the CONEX-Plus programme funded by Universidad Carlos III de Madrid and the European Union's Horizon 2020 research and innovation programme under the Marie Sklodowska-Curie grant agreement No. 801538.

ABSTRACT In this work, a slotted wideband eight-element multiple-input multiple-output (MIMO) antenna system is presented, which covers the N77 (3.2-4.2 GHz) frequency band. The MIMO antennas are printed on a 0.8-mm-thick FR-4 substrate with dimensions of 150 × 75 mm^2. The antennas are placed along the length and width of the printed circuit board (PCB). The arrangement of antenna elements offers pattern and polarization diversity, enhancing the smartphone's ability to receive signals from various directions. The wideband characteristics in the frequency range of 3.25-4.49 GHz are achieved by utilizing a T-slot and an inverted C-slotted stub together. The radiation and total efficiency are found to be >60% for all the MIMO elements. For enhanced isolation between antenna elements placed along the width of the PCB, a slot is introduced, which ensures an isolation of 14.5 dB. This helps achieve an envelope correlation coefficient (ECC) <0.025, diversity gain (DG) >9.95 dB, and a maximum channel capacity (CC) of 40 bps/Hz. The performance of the MIMO antenna is also assessed in the presence of a human, and comparable results are observed. In addition, the examination of the specific absorption rate (SAR) confirms that it remains well within the safety margins when in proximity to humans.

INDEX TERMS Wideband, MIMO, slot antenna, diversity.

I. INTRODUCTION

The rise of 5G technology has revolutionized wireless communication by offering unprecedented speed, capacity, and reliability. A key factor driving this advancement is Multiple-Input Multiple-Output (MIMO) antenna systems utilizing several radiating elements on each end of the connection for improve link reliability, and counteract multipath fading [1], [2]. In sub-6GHz and mmWave frequency spectrum, MIMO elements are crucial. The sub-6GHz spectrum provides wider

The associate editor coordinating the review of this manuscript and approving it for publication was Prakasam Periasamy.

coverage and better penetration through obstacles, while MIMO technology in this range enables higher data rates through spatial multiplexing. Spatial multiplexing allows the simultaneous transmission of multiple data streams, greatly increasing capacity [3], [4]. Additionally, MIMO antennas combat multipath fading by intelligently combining signals received from different antennas, ensuring reliability and overall performance improvement. In order for 5G mobile phones to effectively transmit and receive signals, they typically require 4-8 antenna elements operating at the same frequency to work together [5], [6]. However, because of close proximity of these elements, there is a phenomenon called coupling, which can negatively impact the efficiency of antenna data transmission. It is crucial, therefore, to minimize both the coupling and the ECC between these antenna [7]. To address this issue, the most straightforward decoupling technique involves physically separating the antenna elements, and placing them at sufficient distances from each other. By increasing the spacing between the elements, the near-field coupling and resulting interference can be reduced [8]. Numerous MIMO systems have been put forth in literature. In [9], a MIMO antenna array with eight antennas designed for operation at 3.5 GHz. Every antenna is designed as an Inverted-L monopole encircled by a parasitic structure. The array uses techniques like a neutralization line and a middle slot to minimize interference between the antennas. In [10] a uni-planar loop MIMO system is presented with bandwidth ranging from 3.2-4GHz supporting both vertical and horizontal polarization. The isolation among radiating elements is increased by adding modified arrow-shaped strips. In [11] an eight-element MIMO covering 3.3-4.2 GHz for handheld applications is presented with each antenna made up of a meandered branch self-isolated branch network. In [12] a MIMO system is presented comprising separate antenna pairs integrated within slits of 5G metal-case smartphone incorporating stubs within each of the four slits operating in both N77 (3.3 GHz to 4.2 GHz) and N79 (4.4 GHz to 5.0 GHz) frequency bands. To coupling suppression, a bent stub is incorporated improving isolation up to 11.5 dB and ECC below 0.2. The efficiency falls within the range of 38% to 52%. In [13] an eight-port antenna system using shared square-ring slot radiators is described resonating at 3.3-3.9 GHz. To enhance the isolation, a circular ring, and open-ended passive elements have been added to each square-shaped slot radiator. As a result of this modification, the isolation significantly improved, with an increase of up to 20 dB. In [14] a MIMO system employing inverted L-shaped monopole antennas is discussed. The configuration consists of eight inverted L-shaped elements and L-shaped strips that extend from the ground plane. These passive strips serve as tuning components for four of the inverted L-shaped monopoles positioned along the chassis sides. This arrangement is utilized to effectively extend the electrical dimensions of the antennas, allowing for the attainment of the desired resonance.

This paper presents a slot-based eight-element MIMO system for wideband N77 5G smartphones. The proposed system composed of a T shape slot on the ground plane accompanied by an inverted C shape on the right side of the resonating slot. This inverted C-shaped slotted stub improves the resonating characteristics and improves the efficiency of the system. The MIMO elements are arranged at the horizontal and vertical edges of PCB ensuring both vertical and horizontal polarizations. The minimum isolation is found to be less than 14.5dB and fabricated prototype measurements well agreed with simulations.

II. ANTENNA DESIGN

The MIMO system is designed on 0.8 mm FR4 substrate having a 4.4 permitivitty and 0.002 loss tangent. The board size remained at 150 × 75 mm^2. In Fig.1, the proposed MIMO system is depicted. The feedline was maintained at 2 × 18 mm^2. The DGS slot, as shown in the figure, comprised both T and inverted C shapes. (In Fig.1b, F1-F8 stands for Feed Points.)

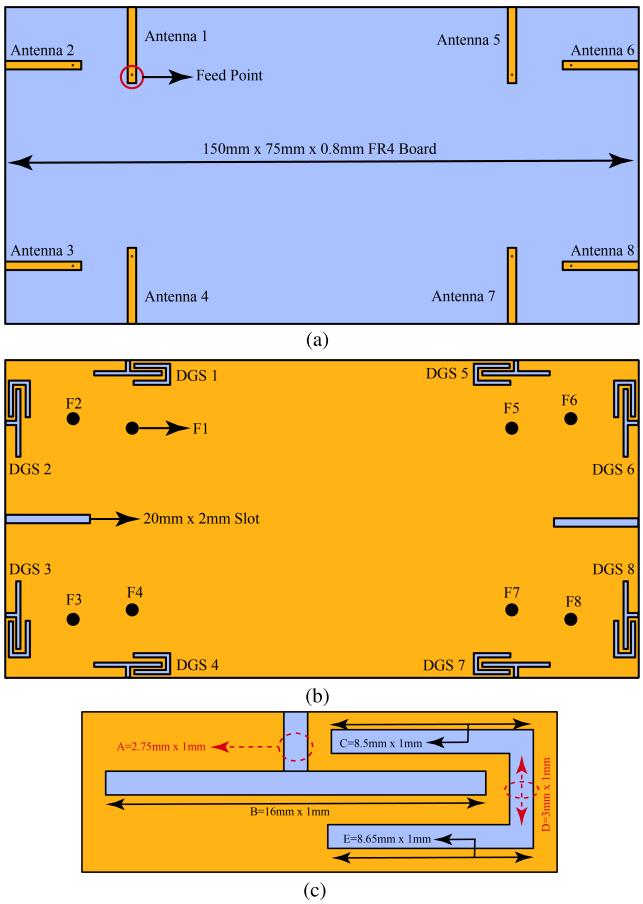

FIGURE 1. Proposed MIMO antenna system (a) Front view (b) Back view (c) Ground slotted stubs.

The design evolution was characterized into three stages, namely Stages 1, 2, and the proposed Stage 3 (refer to Fig.2). In Stage 1, an L-shaped ground slot was introduced, producing resonance at 3.55GHz with a bandwidth ranging

from 3.3 to 3.7GHz. In Design B, the L-shaped DGS was transformed into a T-shaped structure, generating a wideband response from 3.36 to 4.45GHz, thus covering the entire N77 band. In the final design, an inverted C-shaped slotted stub was introduced to enhance the resonance characteristics of the proposed MIMO system. The slot also improved the starting resonance up to 100MHz, and a bandwidth of 3.25 to 4.49GHz was achieved.

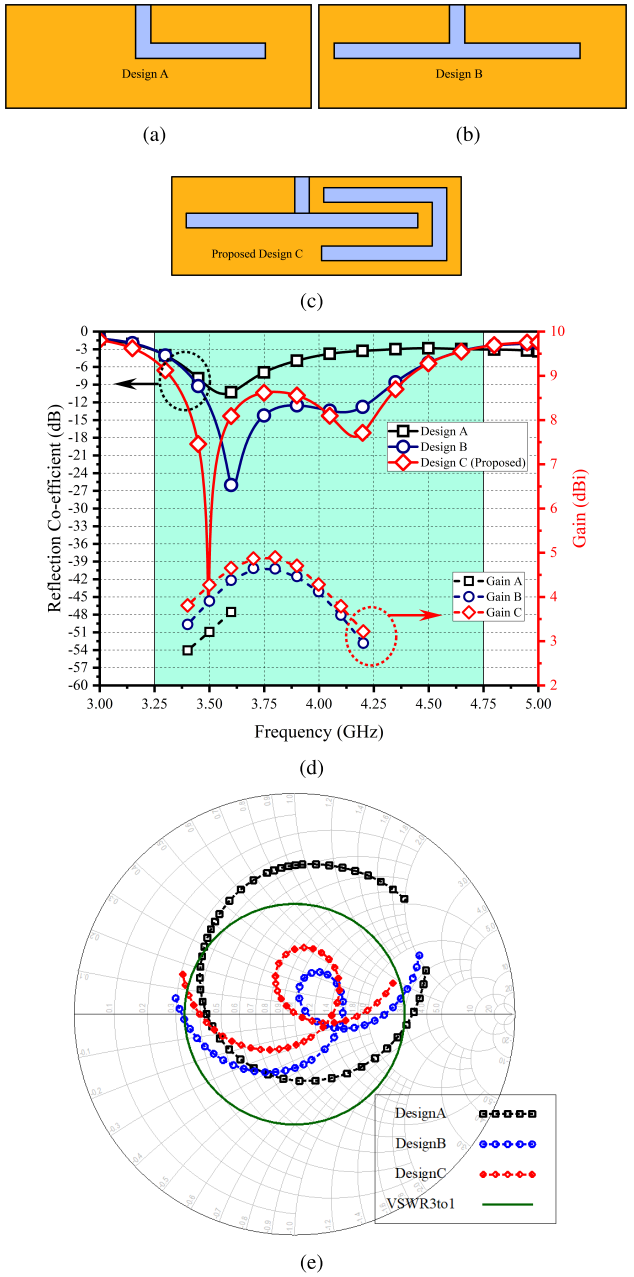

FIGURE 2. (a) Design A (b) Design B (c) Proposed design (d) S-Parameters of design evolution (e) Smith chart of design evolution.

The gain of the proposed antenna at each evolution stage is also shown in Fig.2d. It can be seen that the gain at the proposed and final stage showed maximum value since the antenna input impedance was matched by the

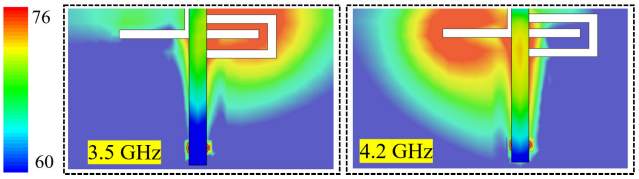

FIGURE 3. Surface current distribution at 3.5 and 4.2GHz.

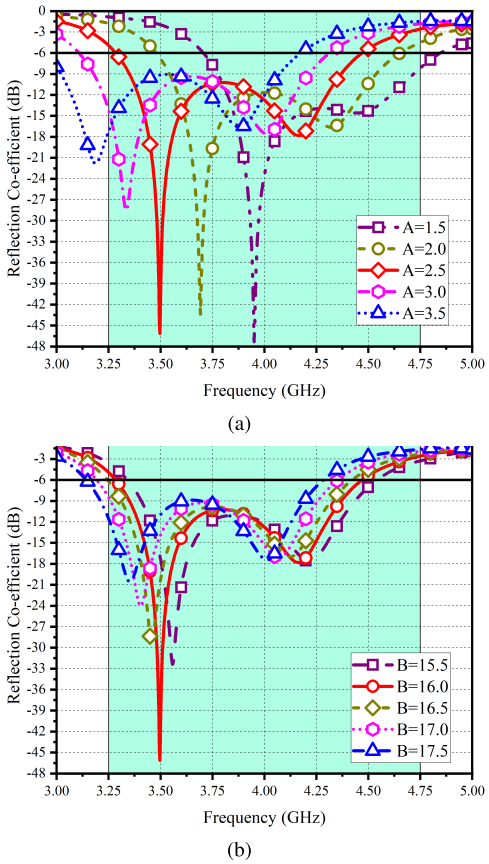

FIGURE 4. Parametric studies of strip (a) A (b) B.

slotted stub that contributed to radiation as a load. The gap between the open stub and the T slot electrically acted as a series capacitor. Looking at Smith Chart in Fig.2e, matching was achieved by increasing the series capacitance by adding the inverted C-slotted stub alongside the T slot. Fig.3, Illustrates the surface current distribution of a solitary antenna. A depiction in the diagram reveals that during the initial resonance, the current primarily accumulates on the right side of the T-shaped slot, and strong coupling concentration is also observed at inverted C slotted stub while at the higher resonances modes, the current concentration is primarily concentrated at the left side of T shape stub showing every side is responsible for generating resonances. The resonance behavioral response of the proposed antenna can be better analyzed by parametrical study. Two primary physical parameters A and B are studied. The observed frequency shifts in the proposed T-shaped stub antenna structure, as depicted in Fig.4a and Fig.4b, are directly

influenced by variations in the two key parameters, A and B. In Fig.4a, where parameter A is adjusted within the range of 1.5mm to 3.5mm, a noteworthy response is noted. Initiating at the lowest value of 1.5mm, the central frequency experiences a pronounced forward shift to 3.9GHz. With a steady incremental increase in A by 0.5mm, the central frequency progressively shifts backward.

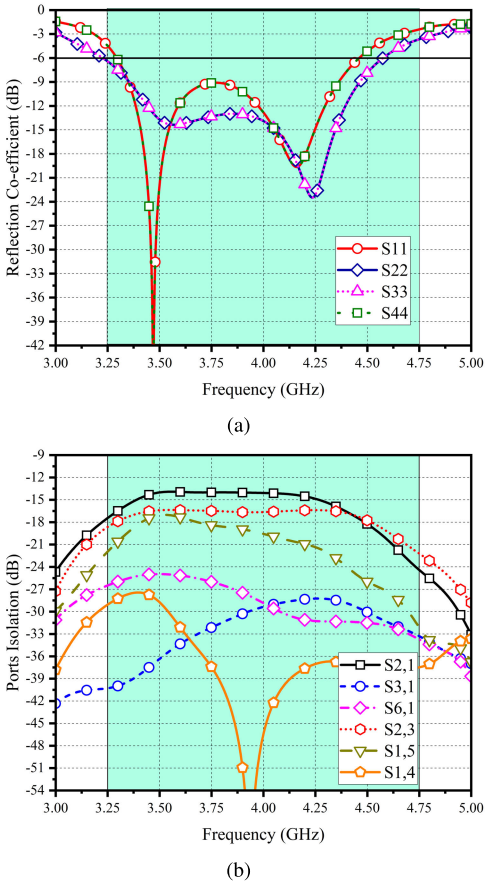

FIGURE 5. S-Parameters simulated (a) Reflection co-efficient and (b) Coupling.

However, beyond the optimal value of 2.5mm, both the resonance response and impedance characteristics exhibit a regression, indicating suboptimal performance. Fig.4b portrays the influence of parameter B on the resonance response. Comparatively, it is observed that, in contrast to parameter A, variations in B have a less substantial effect on the antenna's resonance characteristics. Nevertheless, as the size of parameter B increases, there is still a discernible shift of the resonance frequency to higher levels. It is worth noting that any deviation from the optimum value of B results in impedance mismatch, further emphasizing the sensitivity of the antenna structure to parameter adjustments. In Fig.5 we present the simulated S-Parameters response of the MIMO system under consideration. To maintain simplicity, the analysis focuses on just one side of the MIMO system. The reflection coefficient values from Fig. 5a shows clearly that all radiating elements cover resonance from 3.26-4.48GHz

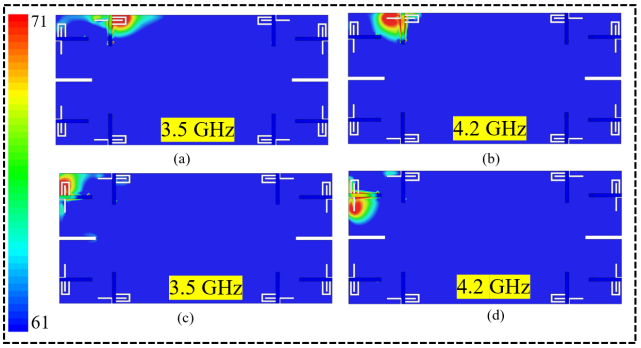

FIGURE 6. Surface current at 3.5 and 4.2GHz (a) (b) Ant 1 (c) and (d) Ant 2.

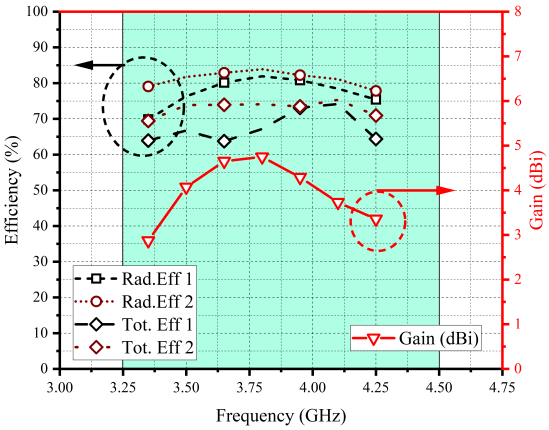

FIGURE 7. Gain and efficiency of MIMO antenna.

hence covering the complete N77 band. The isolation value observe is 14.5dB for adjacent radiating elements and for vertically polarized radiating elements such as Ant 2 and Ant 3, the isolation due to insertion of slotted stub is noted to be 17.5 dB.

The impact of a slot on the behavior of MIMO elements is illustrated through surface currents, as depicted in Fig. 6. In Fig. 6a and b, the currents of Ant 1 at resonance frequencies of 3.5 and 4.2GHz are presented, showing minimal influence on adjacent radiating elements, including Ant 5, owing to their greater separation. Conversely, Fig. 6c and d reveal Ant 2 experiencing significant destructive current interference, attributed to the central slot on neighboring Ant 3.

In Fig.7, the gain and efficiencies of the suggested MIMO system are illustrated, with a focus on Antenna 1 and Antenna 2. The radiation efficiency falls within a range of 70% to 85%, indicating the effectiveness of these antennas in converting input power into radiated energy. Additionally, the total efficiency, which encompasses both radiation and other losses, is observed to vary between 65% and 70%. The gain of the system displays fluctuations from 2.5 to 4.8dB across different frequency points, with a gain value of 4dB at 3.5GHz.

III. RESULT AND DISCUSSIONS

The development and evaluation of MIMO antenna system involved in-house fabrication and testing. The prototype's

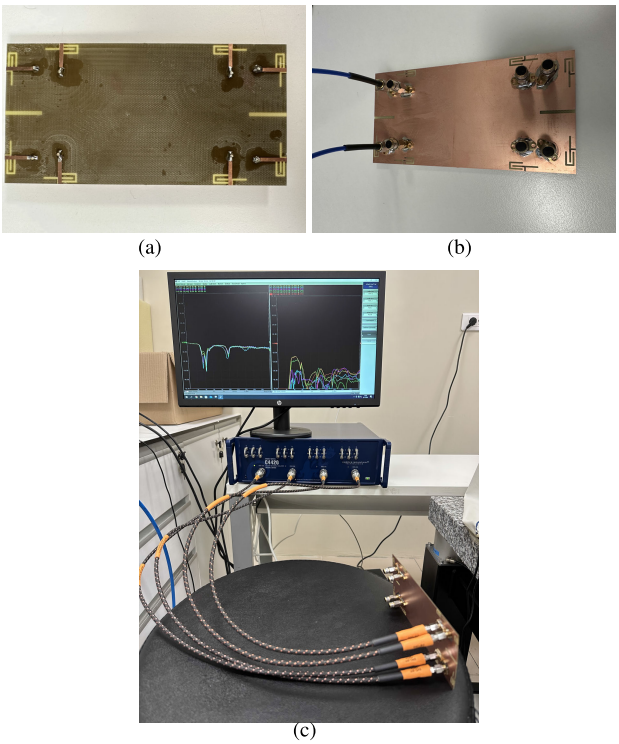

FIGURE 8. Fabricated prototype (a) Front side (b) Back (c) Measurement view.

visual representation, both front and back can be seen in Fig.8.

First, the initial prototype of the proposed antenna model is displayed in its front side, while Fig.8b shows the close view of the backside of the antenna prototype. Subsequently, The measured S-parameters are shown in Fig.9. The reflection coefficient covers the desired bandwidth and well agrees with simulations. In contrast, for port isolation, the measured isolation value is noted to be less than 15 dB. The minor variation observed between the simulated and measured outcomes can be attributed to factors such as fabrication tolerances, losses in coaxial connectors, and other related considerations. The presented MIMO antenna's far-field radiation characteristics are assessed at anechoic chamber. The MIMO antenna is affixed to the back of a wooden rod on a turntable using double-sided tape. Given the array structure's mirror symmetry, the expectation is for antenna elements placed in symmetrical positions in opposing planes to exhibit similar radiation characteristics. To streamline the analysis, our focus is on just one side of the antenna elements, namely Ant1, Ant2, Ant3, and Ant4. Fig.10 and Fig.11 provide visual representations of polar patterns in the *xz* and *yx* planes.

Ant1 and Ant4 at 3.5 GHz on the *yx* plane are noted at 90° and 270°, while for Ant2 and Ant3, the main beam is noted at 59° and 215° with the exception of two nulls. For *xz* plane, Ant1 and Ant4 exhibit butterfly patterns while Ant2 and Ant3 show radiation at 270°. Similarly at 4.2GHz the antenna exhibit pattern diversity characteristics. Due to

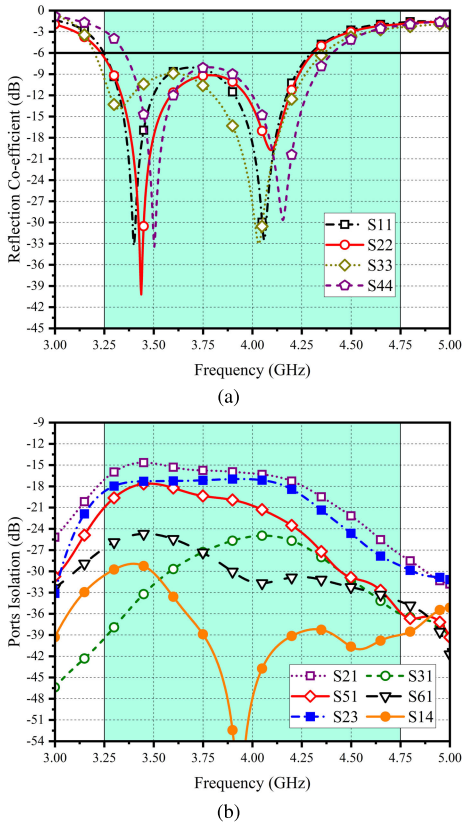

FIGURE 9. Measured S-Parameters (a) Reflection co-efficient and (b) Ports isolation.

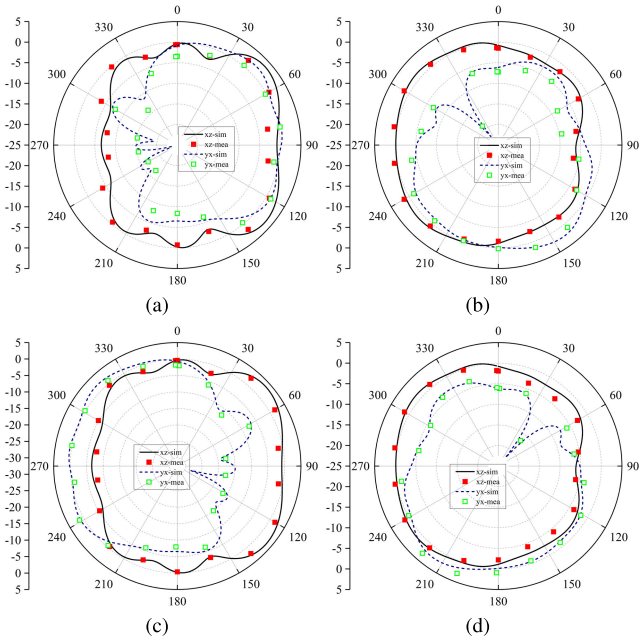

FIGURE 10. Polar radiation plots at 3.5GHz (a) Ant1 (b) Ant2 (c)Ant3 (d)Ant4.

horizontal and vertical placement of MIMO elements, pattern and polarization diversity is achieved. While there are minor discrepancies between the measured and simulated outcomes, the two findings exhibit a broad similarity.

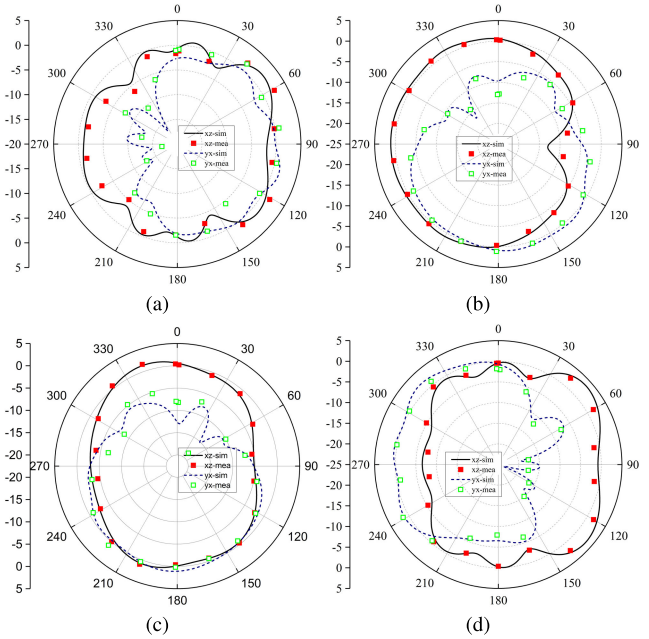

FIGURE 11. Polar radiation plots at 4.2GHz (a) Ant1 (b) Ant2 (c)Ant3 (d)Ant4.

IV. MIMO PARAMETERS

It is essential to evaluate various key parameters for MIMO system. The parameters include the Envelope Co-Relation Coefficient (ECC), Diversity Gain (DG), and Ergodic Channel Capacity (CC).ECC is a crucial metric that indicates the degree of isolation between antennas within the MIMO system. ECC is determined using method descibed in [20] and [21]. ECC values below 0.5 is generally recommended. Fig.12 in our analysis presents a comparison between the ECC values obtained through simulation and those measured in real-world scenarios for the proposed MIMO system.

This graphical representation helps in understanding how well the MIMO system's antennas are isolated.Looking at the graph, we notice that the ECC value remains incredibly low, consistently below 0.035 across the entire operating bandwidth. Specifically, when we consider antenna elements that are positioned facing each other, like Antenna 5 and Antenna 2, the ECC is around 0.035. However, when we look at Antenna 1 and Antenna 2, we see that the ECC is even lower, at 0.025 and sometimes even less. This means that the antennas in these positions exhibit very strong isolation from each other. The DG of MIMO system is found to be in well satisfies limits as seen in Fig.13a (eq 1)

$$DG = 10\sqrt{1 - (ECC^2)} \tag{1}$$

Channel Capacity (CC) was determined through the averaging of 10,000 instances of Rayleigh fading with a fixed SNR reference level at 20 dB. In Fig 13b, the CC of the proposed MIMO system was graphically presented. The plot indicated that CC spanned from 36 to 39.15 bits per second per Hertz (bps/Hz), closely aligning with the desired range.

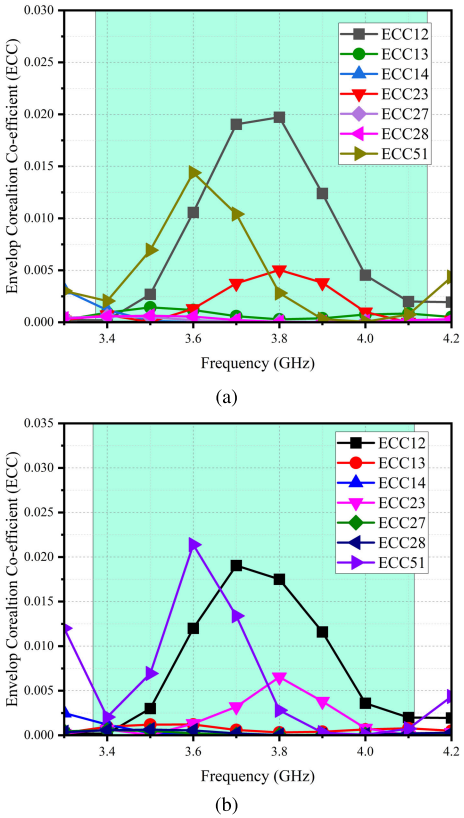

FIGURE 12. ECC (a) simulated and (b) measured.

V. TALK MODE ANALYSIS

Analyzing MIMO antenna parameters like gain and S-parameters is crucial in smartphone design for talk mode scenarios. Gain ensures strong signal reception/transmission, vital for clear voice communication. S-parameters help optimize antenna configurations, minimizing interference and enhancing overall performance. This analysis is essential to ensure smartphones deliver a reliable and high-quality voice communication experience.The S-parameters as illustrated in Fig.14 shows that the radiation elements exhibit similar return loss performances with high impedance matching (around −20 dB reflection coefficients) at 3.5 GHz apart from antenna 2 which can be due to fact that its placed directly below hand phantom but still covering the wideband response. Additionally, Fig. Fig.14b depicts the mutual coupling function, showing values less than −14 dB, indicating good mutual coupling characteristics. This suggests that the antenna elements maintain strong radiation performance, crucial for 5G smartphone applications, where close proximity of antennas demands low mutual coupling to prevent loss of radiation performance.

Fig.15 illustrates the 3D radiation patterns of each element during talk mode, incorporating the user's hand/head presence. The MIMO smartphone antenna system exhibits clear and comprehensive radiation patterns, ensuring wide coverage across various regions. Moreover, the elements maintain satisfactory gain levels in talk mode. To assess its impact on human health, especially during operation

TABLE 1. Comparison with other published work.

Ref	MIMO	Board size (mm^2)	Frequency (GHz)	Port Isolation	Efficiency(%)	ECC
[9]	8	136×68	3.4-3.6	<10	45-60	<0.3
[10]	8	150×75	3.2-4.0	>10	50-75	<0.01
[11]	8	150×75	3.2-4.2	>13	40-70	<0.03
[12]	8	150×75	3.2-4.2/4.4-5.0	>11.5	38-52	<0.03
[13]	8	150×75	3.3-3.9	>19	50-65	<0.02
[14]	8	136×68	3.3-3.7	>14	50-70	<0.02
[15]	8	150×75	3.3-3.6	>15	45-65	<0.05
[16]	8	150×75	3.4-3.6	>15	40-60	<0.15
[17]	8	150×75	3.4-3.6	>12.5	30-59	<0.15
[Prop.]	8	150×75	3.26-4.48	>14.5	60-85	<0.03

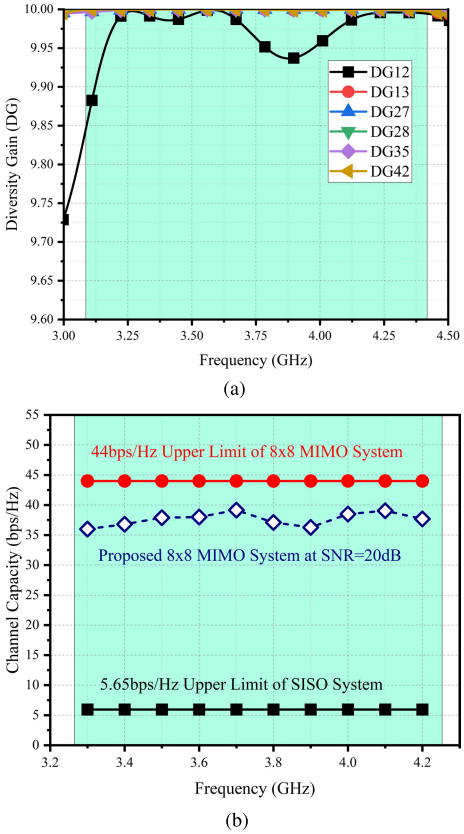

FIGURE 13. Diversity gain and channel capacity of MIMO antenna.

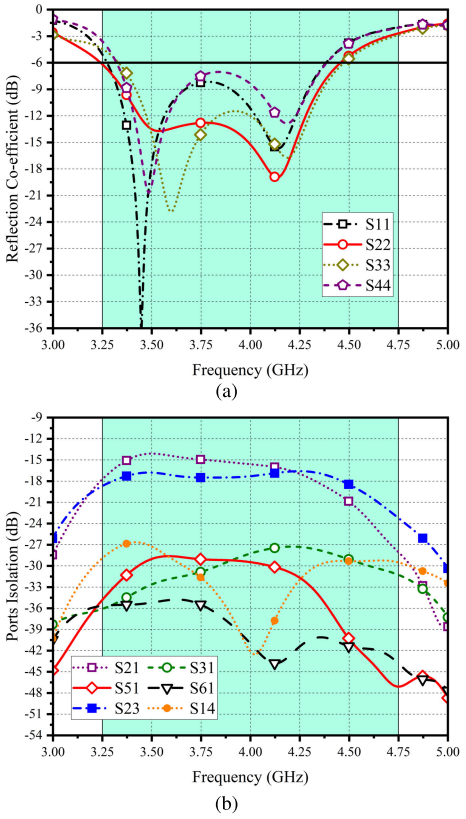

FIGURE 14. S-Parameters in talk mode (a) Reflection co-efficient and (b) Ports isolation.

in both uplink and downlink scenarios, an examination of the SAR was conducted. The need for SAR analysis in smartphone antenna design and performance cannot be overstated. It serves as a vital component in safeguarding both user well-being and device efficiency. SAR analysis plays a pivotal role by quantifying the rate at which human tissues absorb radiofrequency electromagnetic fields emitted by a smartphone during typical usage. Its significance lies in assessing compliance with stringent safety standards, thus protecting users from potentially harmful levels of radiofrequency radiation. Furthermore, this analysis aids in the strategic positioning and design optimization of smartphone antennas, thereby enhancing not only user safety but also the device's overall signal transmission and reception capabilities. In accordance with established standards, SAR values should be below 1.6 W/Kg for a 1-gram tissue and 2 W/Kg for a 10-gram tissue. To calculate SAR in our simulation environment, we positioned the system 2 mm away from model, obtained from a CST library documented properties. Each antenna received an input power of 25 mW, resulting in 200 mW distributed among system. The SAR results for the 1-gram tissue scenario are depicted in Fig. 16. It is evident that the highest SAR value observed was 1.27 W/Kg as displayed in Fig. 16.

A contrast between the MIMO antennas we put forward and those introduced previously is provided in Table 1. The information within the table illustrates that our suggested MIMO antenna demonstrates strong performance attributes,

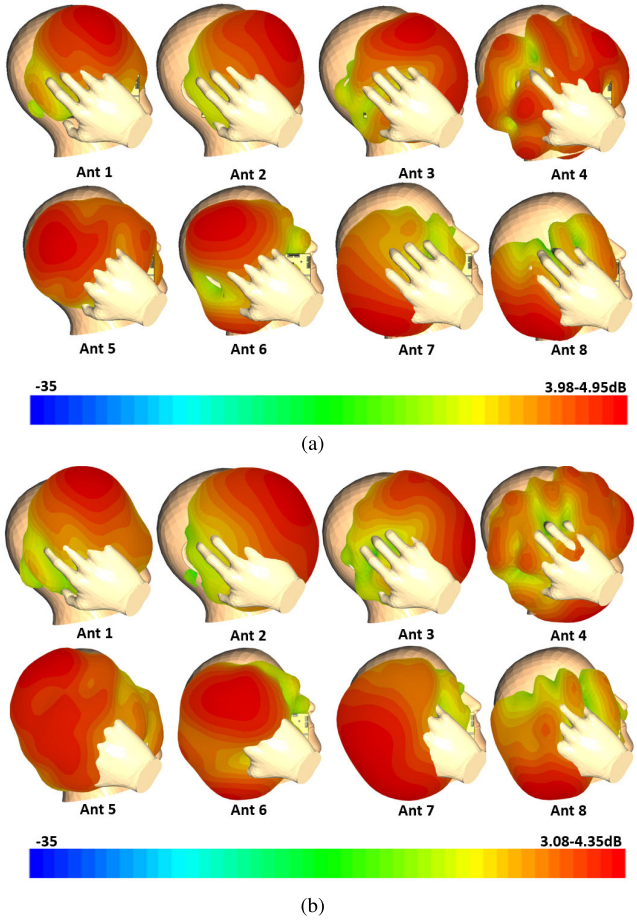

FIGURE 15. 3D Patterns in talk ModeC (a) 3.5GHz and (b) 4.2GHz.

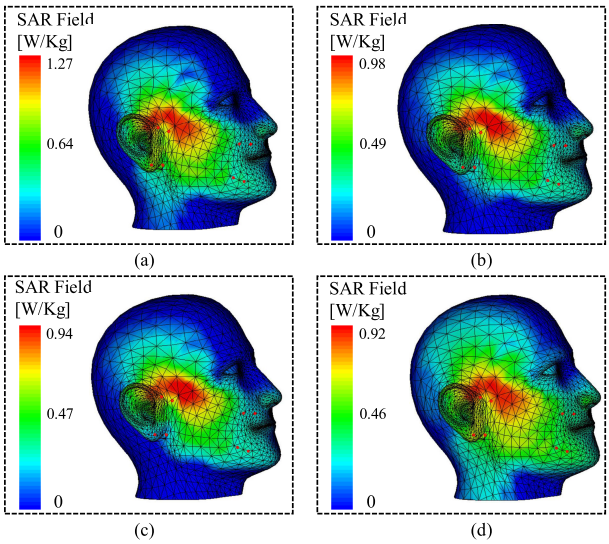

FIGURE 16. SAR analysis of MIMO antenna (a) 3.5GHz (b) 3.7GHz (c) 3.9GHz and (d) 4.2GHz.

featuring minimal Envelope Correlation Coefficients (ECC) and elevated Channel Capacity (CC) values.

VI. CONCLUSION

This study presents an economical, straightforward, and adaptable wideband MIMO antenna system intended for use in smartphones, specifically operating at sub 10 GHz frequencies. The system is constructed on an FR4 substrate, with the primary board dimensions measuring 150 × 75 × 0.8 mm^3. It exhibits resonance at 3.26 GHz and 4.38 GHz, offering a −6 dB bandwidth of 1.12 GHz while maintaining a minimum isolation of −14.5 dB between antenna elements. Noteworthy features encompass a peak gain of 4.8 dBi, low Envelope Correlation Coefficient (ECC) (<0.03), efficiency levels ranging from 60% to 85%, a peak Specific Absorption Rate (SAR) of 1.27 W/Kg, and a maximum Channel Capacity (CC) of 39.15 bits per second per Hertz (bps/Hz) within the desired frequency range. The study includes a brief survey of existing literature and a comparison with prior research. A prototype was constructed and subjected to testing, demonstrating a robust agreement between the simulated and observed results. These outcomes suggest a promising future for the integration of this antenna system in the next generation of intelligent mobile devices.

REFERENCES

[1] M. Farasat, D. N. Thalakotuna, Z. Hu, and Y. Yang, "A review on 5G sub-6 GHz base station antenna design challenges," *Electronics*, vol. 10, no. 16, p. 2000, Aug. 2021.
[2] A. Goudarzi, M. M. Honari, and R. Mirzavand, "Resonant cavity antennas for 5G communication systems: A review," *Electronics*, vol. 9, no. 7, p. 1080, Jul. 2020.
[3] S. H. Kiani, A. Iqbal, S.-W. Wong, H. S. Savci, M. Alibakhshikenari, and M. Dalarsson, "Multiple elements MIMO antenna system with broadband operation for 5th generation smart phones," *IEEE Access*, vol. 10, pp. 38446–38457, 2022.
[4] K. Sultan, M. Ikram, and N. Nguyen-Trong, "A multiband multibeam antenna for sub-6 GHz and mm-wave 5G applications," *IEEE Antennas Wireless Propag. Lett.*, vol. 21, no. 6, pp. 1278–1282, Jun. 2022.
[5] G. Kim and S. Kim, "Design and analysis of dual polarized broadband microstrip patch antenna for 5G mmWave antenna module on FR4 substrate," *IEEE Access*, vol. 9, pp. 64306–64316, 2021.
[6] S. H. Kiani, H. S. Savci, H. S. Abubakar, N. O. Parchin, H. Rimli, and B. Hakim, "Eight element MIMO antenna array with tri-band response for modern smartphones," *IEEE Access*, vol. 11, pp. 44244–44253, 2023, doi: 10.1109/ACCESS.2023.3271716.
[7] W. An, Y. Li, H. Fu, J. Ma, W. Chen, and B. Feng, "Low-profile and wideband microstrip antenna with stable gain for 5G wireless applications," *IEEE Antennas Wireless Propag. Lett.*, vol. 17, no. 4, pp. 621–624, Apr. 2018.
[8] Y. Yang, J. Ren, B. Zhang, J. Liu, H. Wang, D. Song, and Y. Yin, "Wideband tripolarized MIMO antenna with pattern diversity for 5G application," *IEEE Antennas Wireless Propag. Lett.*, vol. 23, no. 1, pp. 349–353, Jan. 2024, doi: 10.1109/lawp.2023.3324391.
[9] M. Abdullah, Y.-L. Ban, K. Kang, M.-Y. Li, and M. Amin, "Eight-element antenna array at 3.5 GHz for MIMO wireless application," *Prog. Electromagn. Res. C*, vol. 78, pp. 209–216, 2017, doi: 10.2528/pierc17082308.
[10] N. O. Parchin, H. J. Basherlou, Y. I. A. Al-Yasir, and R. A. Abd-Alhameed, "A broadband multiple-input multiple-output loop antenna array for 5G cellular communications," *AEU - Int. J. Electron. Commun.*, vol. 127, Dec. 2020, Art. no. 153476.
[11] A. Zhao, Z. Ren, and S. Wu, "Broadband MIMO antenna system for 5G operations in mobile phones," *Int. J. RF Microw. Comput.-Aided Eng.*, vol. 29, no. 10, Oct. 2019, Art. no. e21857, doi: 10.1002/mmce.21857.
[12] J. Ahn, Y. Youn, B. Kim, J. Lee, N. Choi, Y. Lee, G. Kim, and W. Hong, "Wideband 5G N77/N79 4 × 4 MIMO antenna featuring open and closed stubs for metal-rimmed smartphones with four slits," *IEEE Antennas Wireless Propag. Lett.*, vol. 22, no. 12, pp. 2798–2802, Dec. 2023, doi: 10.1109/lawp.2023.3297990.
[13] N. O. Parchin, Y. I. A. Al-Yasir, A. H. Ali, I. Elfergani, J. M. Noras, J. Rodriguez, and R. A. Abd-Alhameed, "Eight-element dual-polarized MIMO slot antenna system for 5G smartphone applications," *IEEE Access*, vol. 7, pp. 15612–15622, 2019, doi: 10.1109/ACCESS.2019.2893112.

[14] M. Abdullah, A. Altaf, M. R. Anjum, Z. A. Arain, A. A. Jamali, M. Alibakhshikenari, F. Falcone, and E. Limiti, "Future smartphone: MIMO antenna system for 5G mobile terminals," *IEEE Access*, vol. 9, pp. 91593–91603, 2021, doi: 10.1109/ACCESS.2021.3091304.
[15] K.-L. Wong, C.-Y. Tsai, and J.-Y. Lu, "Two asymmetrically mirrored gap-coupled loop antennas as a compact building block for eight-antenna MIMO array in the future smartphone," *IEEE Trans. Antennas Propag.*, vol. 65, no. 4, pp. 1765–1778, Apr. 2017.
[16] W. Jiang, B. Liu, Y. Cui, and W. Hu, "High-isolation eight-element MIMO array for 5G smartphone applications," *IEEE Access*, vol. 7, pp. 34104–34112, 2019.
[17] L. Chang, Y. Yu, K. Wei, and H. Wang, "Polarization-orthogonal co-frequency dual antenna pair suitable for 5G MIMO smartphone with metallic bezels," *IEEE Trans. Antennas Propag.*, vol. 67, no. 8, pp. 5212–5220, Aug. 2019.
[18] N. Ojaroudi Parchin, H. Jahanbakhsh Basherlou, Y. I. A. Al-Yasir, A. M. Abdulkhaleq, M. Patwary, and R. A. Abd-Alhameed, "A new CPW-fed diversity antenna for MIMO 5G smartphones," *Electronics*, vol. 9, no. 2, p. 261, Feb. 2020.
[19] N. O. Parchin, J. Zhang, R. A. Abd-Alhameed, G. F. Pedersen, and S. Zhang, "A planar dual-polarized phased array with broad bandwidth and quasi-endfire radiation for 5G mobile handsets," *IEEE Trans. Antennas Propag.*, vol. 69, no. 10, pp. 6410–6419, Oct. 2021, doi: 10.1109/TAP.2021.3069501.
[20] P. Jha, A. Kumar, A. De, and R. K. Jain, "Modified CSRR based dual-band four-element MIMO antenna for 5G smartphone communication," *Prog. Electromagn. Res. Lett.*, vol. 101, pp. 35–42, 2021.
[21] P. Jha, A. Kumar, and A. De, "Two-port miniaturized textile antenna for 5G and WLAN applications," *Int. J. Microw. Wireless Technol.*, vol. 15, no. 8, pp. 1443–1452, Oct. 2023.

SAAD HASSAN KIANI received the B.S. degree from the City University of Science and Information Technology, in 2014, the M.S. degree from Iqra National University, in 2018, and the Ph.D. degree from the IIC University of Technology, Cambodia, in 2022. He was a part of the Smart Systems Engineering Laboratory, College of Engineering, Prince Sultan University, Saudi Arabia, from July 2022 to January 2023. He is currently a Research Scientist with the RFMicroSense Research Group, Istanbul Medipol University, İstanbul, Turkey, and Advance Electromagnetics Research Group, King Abdulaziz University, Jeddah, Saudi Arabia. His research interests include MIMO antenna systems, slot antennas, origami and kirigami antennas, multiband antennas, and metasurfaces.

MEHR E. MUNIR received the B.Sc. degree (Hons.) in electrical engineering (telecommunication engineering) from the City University of Science and Information Technology (CUSIT), Peshawar, Pakistan, in 2014, and the M.Sc. and Ph.D. degrees in electrical engineering (communication and electronics) from Iqra National University (INU), Peshawar, in 2017 and 2023, respectively. He started his career, in February 2015, as a Visiting Lecturer with the Electrical Engineering Department, CUSIT, after that he joined INU, in September 2015, as a Lab Engineer of the Electrical Engineering Department. In November 2018, due to best performance and excellent research profile he promoted to the position of a Lecturer of the Electrical Engineering Department, INU, where he was appointed as a Postgraduate Program Coordinator/a Lecturer of the Electrical Engineering Department, in January 2019. In May 2019, he was appointed as a Senior Design Officer with Aircraft Rebuilt Factory (ARF), Aviation Design Institute (AvDI), Pakistan Aeronautical Complex (PAC), Kamra, Pakistan. Currently, he is a Research Fellow with the Smart System Engineering Laboratory, College of Engineering, Prince Sultan University (PSU), Riyadh, Saudi Arabia.

HÜSEYIN ŞERIF SAVCI (Senior Member, IEEE) received the B.S. degree in electronics and communication engineering from Yıldız Technical University, İstanbul, Turkey, in 2001, and the M.S. and Ph.D. degrees in electrical engineering from Syracuse University, Syracuse, NY, USA, in 2005 and 2008, respectively. His dissertation on Low Power CMOS Receiver for Medical Implant Devices was a recipient of the Best Thesis Award. From 2008 to 2013, he was with Skyworks Solutions Inc., Cedar Rapids, IA, USA, as a Senior RFIC Design Engineer. Between 2013 and 2020, he worked with Hittite Microwave Corporation, Chelmsford, Massachusetts, and Analog Devices Inc., İstanbul, as a Principal Design Engineer. Over the years, he designed and released many RFIC and MMIC products on CMOS, SiGe, SOI, GaN, and GaAs technologies. In 2020, he joined the Department of Electrical and Electronics Engineering, Istanbul Medipol University, İstanbul, as an Assistant Professor. He established the RFMicroSense Research Group, where he conducts research on the design and modeling of RF and microwave integrated circuits, devices, systems, and antennas. He is also serving as an Associate Editor for the *Applied Computational Electromagnetics Society*.

HATEM RMILI (Senior Member, IEEE) received the B.S. degree in physics from the Science Faculty of Monastir, Tunisia, in 1995, the D.E.A. Diploma (master's) degree in quantum mechanics from the Science Faculty of Tunis, Tunisia, in 1999, and the Ph.D. degree in physics (electronics) from the University of Bordeaux 1, France, in 2004. From December 2004 to March 2005, he was a Research Assistant with the PIOM Laboratory, University of Bordeaux 1. From March 2005 to March 2007, he was a Postdoctoral Fellow with Rennes Institute of Electronics and Telecommunications, France. From March to September 2007, he was a Postdoctoral Fellow with the ESEO Engineering School, Angers, France. From September 2007 to August 2012, he was an Assistant Professor with the Department of Electronics and Telecommunications, Mahdia Institute of Applied Science and Technology (ISSAT), Tunisia. Currently, he is a Professor with the Electrical and Computer Engineering Department, Faculty of Engineering, King Abdulaziz University, Jeddah, Saudi Arabia. His research interests include applied electromagnetic applications, including antennas, metamaterials, and metasurfaces. The main targeted applications are reconfigurable antennas for multi-standard wireless communications systems, security of chipless RFID systems with fractal tags, terahertz photoconductive antennas for infra-red energy harvesting, UWB nano rectennas for collection of solar energy, phase shifters for low-cost 5G communication systems, and microwave absorbing materials for stealth technologies.

EATEDAL ALABDULKREEM received the Ph.D. degree in computer science from Brunel University. She is currently an Associate Professor with the Department of Computer Sciences, College of Computer and Information Sciences, Princess Nourah bint Abdulrahman University, Riyadh, Saudi Arabia. Her research interests include artificial intelligence, cognitive computing, and networks. She has published several research articles in her field.

HELA ELMANNAI received the Ph.D. degree in information technology from SUPCOM, Tunisia. She is currently an Assistant Professor with the Department of Information Technology, College of Computer and Information Sciences, Princess Nourah bint Abdulrahman University, Saudi Arabia. Her research interests include artificial intelligence, networking, blockchain, and engineering applications.

GIOVANNI PAU (Senior Member, IEEE) received the bachelor's degree in telematic engineering from the University of Catania, Italy, and the master's degree (cum laude) in telematic engineering and the Ph.D. degree from the Kore University of Enna, Italy. He is currently an Associate Professor with the Faculty of Engineering and Architecture, Kore University of Enna. He is the author/coauthor of more than 80 refereed articles published in journals and conference proceedings. He is a member of the IEEE (Italy Section) and he has been involved in several international conferences as the session co-chair and a technical program committee member. He serves/served as a leading guest editor in special issues of several international journals and he is an Editorial Board Member as an Associate Editor of several journals, such as IEEE Access, *Wireless Networks* (Springer), *EURASIP Journal on Wireless Communications and Networking* (Springer), *Wireless Communications and Mobile Computing* (Hindawi), *Sensors* (MDPI), and *Future Internet* (MDPI). His research interests include wireless sensor networks, fuzzy logic controllers, intelligent transportation systems, the Internet of Things, smart homes, and network security.

MOHAMMAD ALIBAKHSHIKENARI (Member, IEEE) was born in Mazandaran, Iran, in February 1988. He received the Ph.D. degree with European Label in electronics engineering from the University of Rome "Tor Vergata," Italy, in February 2020. From May 2018 to December 2018, he was a Ph.D. Visiting Researcher with the Chalmers University of Technology, Gothenburg, Sweden. His training during this Ph.D. research visit included a research stage with Swedish Company Gap Waves, AB, Gothenburg. Since July 2021, he has been with the Department of Signal Theory and Communications, Universidad Carlos III de Madrid (uc3m), Spain, as a Principal Investigator of the CONEX (CONnecting EXcellence)-Plus Talent Training Program and Marie Skłodowska-Curie Actions. He was also a Lecturer of the Electromagnetic Fields and Electromagnetic Laboratory, Department of Signal Theory and Communications, from 2021 to 2022. He received the "Teaching Excellent Acknowledgement" Certificate for the course of electromagnetic fields from the Vice-Rector of studies of uc3m. From December 2022 to May 2023, he spent three industrial and academic research visits in SARAS Technology Ltd., Leeds, England; Edinburgh Napier University, Edinburgh, Scotland; and University of Bradford, West Yorkshire, England, which were defined by CONEX-Plus Talent Training Program and Marie Skłodowska-Curie Actions as his secondment research visit plans. His research interests include electromagnetic systems, antennas and wave-propagations, metamaterials and metasurfaces, sensors, synthetic aperture radars (SAR), 5G and beyond wireless communications, multiple input multiple output (MIMO) systems, RFID tag antennas, substrate integrated waveguides (SIWs), impedance matching circuits, microwave components, millimeter-waves and terahertz integrated circuits, gap waveguide technology, beamforming matrix, and reconfigurable intelligent surfaces (RIS), which led to achieve more than 5400 citations and H-index above 46 reported by Scopus, Google Scholar, and ResearchGate. He was a recipient of the three years Principal Investigator Research Grant funded by Universidad Carlos III de Madrid and the European Union's Horizon 2020 Research and Innovation Program under the Marie Skłodowska-Curie Grant started, in July 2021, the two years Postdoctoral Research Grant funded by the University of Rome "Tor Vergata" started, in November 2019, the three years Ph.D. Scholarship funded by the University of Rome "Tor Vergata" started, in November 2016, and the two Young Engineer Awards of the 47th and 48th European Microwave Conference were held in Nuremberg, Germany, in 2017, and Madrid, Spain, in 2018, respectively. In April 2020, his research article titled "High-Gain Metasurface in Polyimide On-Chip Antenna Based on CRLH-TL for Sub Terahertz Integrated Circuits" published in Scientific Reports was awarded as the Best Month Paper at the University of Bradford. He is serving as an Associate Editor for *Radio Science* and *IET Journal of Engineering*. He also acts as a referee in several highly reputed journals and international conferences.

Open Access funding provided by 'Università degli Studi di Enna "KORE"' within the CRUI CARE Agreement